Acquisition of TCF3 and CCND3 Mutations and Transformation to Burkitt Lymphoma in a Case of B-Cell Prolymphocytic Leukemia

M'boyba Diop, Florence Nguyen-Khac, Simon Bouzy, Damien Roos-Weil, Clotilde Bravetti, Agathe Maillon, M 'Boyba Diop, Cécile Doualle, Nathalie Droin, Olivier Bernard, et al.

Acquisition of *TCF3* and *CCND3* Mutations and Transformation to Burkitt Lymphoma in a Case of B-Cell Prolymphocytic Leukemia

Florence Nguyen-Khac[1,2], Simon Bouzy[3], Damien Roos-Weil[2,4], Clotilde Bravetti[1,2], Agathe Maillon[1], M'boyba Diop[5], Cécile Doualle[2], Nathalie Droin[5], Olivier A. Bernard[6,7], Elise Chapiro[1,2]

Correspondence: Elise Chapiro (elise.chapiro@aphp.fr); Florence Nguyen-Khac (florence.nguyen-khac@aphp.fr).

B-cell prolymphocytic leukemia (B-PLL) is a very rare disease; it accounts for <1% of all chronic B-cell leukemias. According to the World Health Organization's definition, B-PLL is diagnosed when peripheral blood (PB) prolymphocytes account for more than 55% of lymphoid cells in a de novo context. B-PLL generally occurs in elderly people presenting B symptoms, a rapidly rise in the lymphocyte count, massive splenomegaly but little or no lymphadenopathy. There are no specific genetic abnormalities; B-PLL has genomic similarities with other chronic B-cell malignancies but displays well-defined combinations of alterations. The karyotype is frequently complex. *MYC* aberrations resulting from mutually exclusive translocations or gains are observed in about 75% of cases. These translocations place the *MYC* gene under the control of an enhancer (usually immunoglobulin genes *IGH*, *IGK*, or *IGL* enhancers) and lead to *MYC* overexpression. Deletions of the short arm of chromosome 17 including the *TP53* gene (del(*TP53*)) are also frequent. *TP53*, *MYD88*, *BCOR*, *MYC*, *SF3B1*, *SETD2*, *CHD2*, *CXCR4*, and *BCLAF1* are the most frequently mutated genes in B-PLL. We recently reported on 3 subgroups in which the prognosis depended on the *MYC* and *TP53* status. Patients with both a *MYC* aberration and del(*TP53*) belong to the high-risk subgroup and have a short mean overall survival time.[1]

Burkitt lymphoma (BL) is an aggressive mature B-cell lymphoma that occurs in adults and children. BL is subdivided into a sporadic subtype (often diagnosed in developed countries, accounting for ~1% of adult lymphomas and ~30% of pediatric lymphomas), the Epstein-Barr-virus-associated endemic subtype, and an HIV-associated subtype. This lymphoma comprises medium-sized monomorphic B-cells with round nuclei, finely clumped chromatin, and deeply basophilic cytoplasm that usually contains lipid vacuoles, numerous mitoses, and tingible body macrophages with a "starry sky" appearance. Although BL characteristic morphology and immunophenotype often enable a rapid diagnosis, testing for genomic aberrations is needed to differentiate BL from other high-grade B-cell neoplasms. Although *MYC* rearrangements are not specific for BL, they are considered as a hallmark feature and are found in almost all cases. The typical t(8;14)(q24;q32) rearrangement (*MYC-IGH*) occurs in 80% of cases. Rearrangements involving the light chain loci *IGL* t(2;8) or *IGK* t(8;22) are less frequent.[2] *MYC* is also the most frequently mutated gene in BL (in 70% of cases). Mutations in the transcription factor 3 (*TCF3*) gene or its negative regulator *ID3* have been reported in about 70% of sporadic subtypes. The other frequently mutated genes are *CCND3*, *TP53*, *RHOA*, *SMARCA4*, and *ARID1A*.[3–5]

Here, we describe a case of concomitant B-PLL and BL. Cytogenetic and molecular analyses revealed a common origin, with the acquisition of additional genetic lesions in the BL clone.

A 46-year-old woman with an unremarkable medical history presented with hyperleukocytosis and thrombocytopenia but no splenomegaly or lymphadenopathy. The white blood cell count was 14.1×10^9/L with 79% lymphocytes, the hemoglobin level was 96g/L, and the platelet count was 25×10^9/L. In a blood smear examination prolymphocytes accounted for 72% of lymphoid cells. Flow cytometry of PB cells revealed a CD5+CD23- CD79b-FMC7+IgMλ^weak clonal B-lymphocyte population. The karyotype (K) was 46,XX,t(8;22)(q24;q11)[2]/46,XX[34]. fluorescence in situ hybridization (FISH) analyses confirmed the t(8;22) with *MYC* rearrangement in 52% of the nuclei and revealed a cryptic del(*TP53*) in 71% of the nuclei. Cohybridization with *MYC* and *TP53* FISH probes showed that 55% of the cells harbored both abnormalities, and 18% had a del(*TP53*) only; hence, the *MYC* translocation had occurred after the del(*TP53*). Our diagnosis was de novo B-PLL. A bone marrow (BM) aspirate showed a massive infiltration by BL cells (accounting for 87% of the BM cells). The clonal BM B-cells' immunophenotype

[1]Service d'Hématologie Biologique, Hôpital Pitié-Salpêtrière, Assistance Publique-Hopitaux de Paris, France
[2]Sorbonne Université, Centre de Recherche des Cordeliers, Inserm, Université de Paris, Cell Death and Drug Resistance in Lymphoproliferative Disorders Team, Paris, France
[3]Service d'Hématologie Biologique, Centre Hospitalo-Universitaire de Rennes, France
[4]Service d'Hématologie Clinique, Hôpital Pitié-Salpêtrière, Assistance Publique-Hopitaux de Paris, France
[5]Analyse moléculaire, modélisation et imagerie de la maladie cancéreuse, INSERM US23/Centre National de la Recherche Scientifique UMS3655, Gustave Roussy, Villejuif, France
[6]INSERM, U1170, Institut Gustave Roussy, Villejuif, France
[7]Université Paris-Sud/Paris Saclay, Orsay, France
Supplemental digital content is available for this article.

was CD5$^-$CD10$^+$bcl2$^-$IgMλ^{high}. The K was 46,X,-X,t(8;22) (q24;q11),der(13)t(7;13)(q21;q34),+20[19]/46,XX[1], and a FISH analysis detected a *MYC* rearrangement and a del(*TP53*) in 59% and 84% of the nuclei, respectively. *IGHV* sequencing in PB and BM samples showed that both displayed the same VH3-21/DH3-10/JH6 recombination, with full sequence identity. The sequences contained somatic mutations (96.9% homology with the germline counterparts). The patient was diagnosed with medullar BL clonally related to B-PLL. After treatment with a cyclophosphamide/oncovin/adriamycin/prednisolone/methotrexate regimen, the patient achieved a complete response in the BM but prolymphocytic cells persisted in the PB. She relapsed 5 months later, with massive BL cell invasion of the BM. An allogeneic BM transplant was performed but she died 1 month later, following BL relapse.[6]

To further investigate the clonal relationship between the B-PLL and BL cells, we performed whole exome sequencing (WES) on DNA extracted from sorted CD19+CD5+ PB tumor cells, BM cells, and sorted nontumor CD3+ PB cells (considered to be germinal controls) sampled at the time of diagnosis. Somatic coding mutations were confirmed by polymerase chain reaction-based targeted deep resequencing (See Supplemental Digital Content, http://links.lww.com/HS/A154). In the PB sample, 19 genes were mutated and the variant allele frequency (VAF) ranged from 29.9% to 95.83%; these included *TP53* (c.T824A, p.L275Q, VAF: 95.83%); *CHD2* (c.4160_4178del, p.P1387Rfs*13, VAF: 47.06%), and *SETD2* (c.2628_2629insAG, p.G878Qfs*14, VAF: 34.88%). The same 19 mutations were present in the BM sample, with similar VAFs. Twenty-seven additional mutations were detected in the BM, including *TCF3* (c.G1663C, p.E555Q, VAF: 40.53%) and *CCND3* (c.T875A, p.L292Q, VAF: 37.25%) (Supplemental Digital Content, Table 1, http://links.lww.com/HS/A155). The copy number aberration analysis from WES data confirmed the chromosomal abnormalities observed by K/FISH, and detected cryptic 17q gain and 14q loss in the PB, and 17q gain and 11q loss in the BM (Figure 1; Supplemental Digital Content, Table 2, http://links.lww.com/HS/A154).

This case provided an unusual illustration of a dual B-cell neoplasm, with B-PLL in the PB and BL in the BM. The B-PLL cells harbored a translocation that deregulates *MYC* expression and had biallelic inactivation of *TP53* (by deletion and mutation); these are the 2 most prevalent abnormalities in B-PLL and, when combined, confer a poor prognosis. Mutations in *CHD2* and *SETD2* (involved in chromatin remodeling) are also frequent in B-PLL.[1] The medullar BL cells carried the same somatic mutations, chromosomal abnormalities and *VDJ* recombination (using the *IGHV3-21* gene) as the B-PLL cells but also had other genetic lesions. *IGHV3* is the predominant subgroup in both BL and B-PLL cells.[1,7] Our results demonstrate that the B-PLL and BL cells had the same clonal origin and suggest strongly that the BL developed from the B-PLL (Figure 2).

The transformation of a chronic B lymphoproliferative disease into an aggressive lymphoma is well known in chronic lymphocytic leukemia (CLL, as Richter's syndrome [RS]), follicular lymphoma (FL), and marginal zone B-cell lymphoma of mucosa-associated lymphoid tissue lymphomas (MALT) but has not been described previously in B-PLL. Our case is unique in this respect. In CLL, RS occurs in 2%–8% of patients. Most frequently, clonally related (80%) or unrelated (20%) diffuse large B-cell lymphoma (DLBCL) develops, whereas transformation to classical Hodgkin lymphoma is rare.[8] Transformation to BL is very unusual in CLL; only a few cases have been reported.[9–11] Transformation is linked to the acquisition of additional chromosomal abnormalities and somatic mutations. In DLBCL-type RS, genetic lesions typically affect the *TP53*, *NOTCH1*, *MYC*, and *CDKN2A* genes. The *MYC* network is deregulated in ~70% of samples.[8] *MYC* pathway deregulation is also considered to be a key event in transformation of MALT (40%–80% of cases) and FL (~40%) to DLBCL, and is often associated with *TP53* aberrations.[12,13] In our case, transformation to BL was not due to *MYC* deregulation or *TP53* inactivation alone because these aberrations were already present in the B-PLL cells. Moreover, *MYC* deregulation is known to be insufficient for BL oncogenesis. Additional genetic lesions cooperate with *MYC* to generate human BL.[14] The additional mutations observed in our patient's BM included mutations in the *TCF3* and *CCND3* genes, both of which are frequently mutated in de novo BL. The L292Q *CCND3* missense mutation, novel in BL, affects a
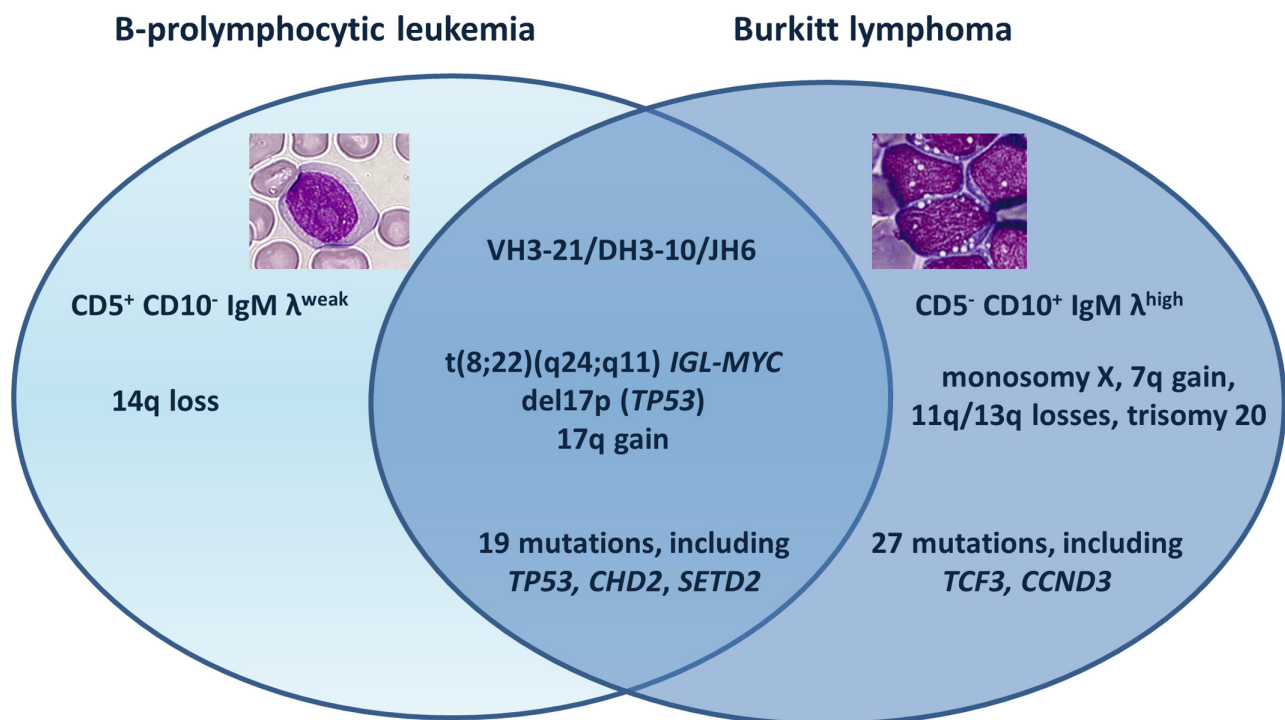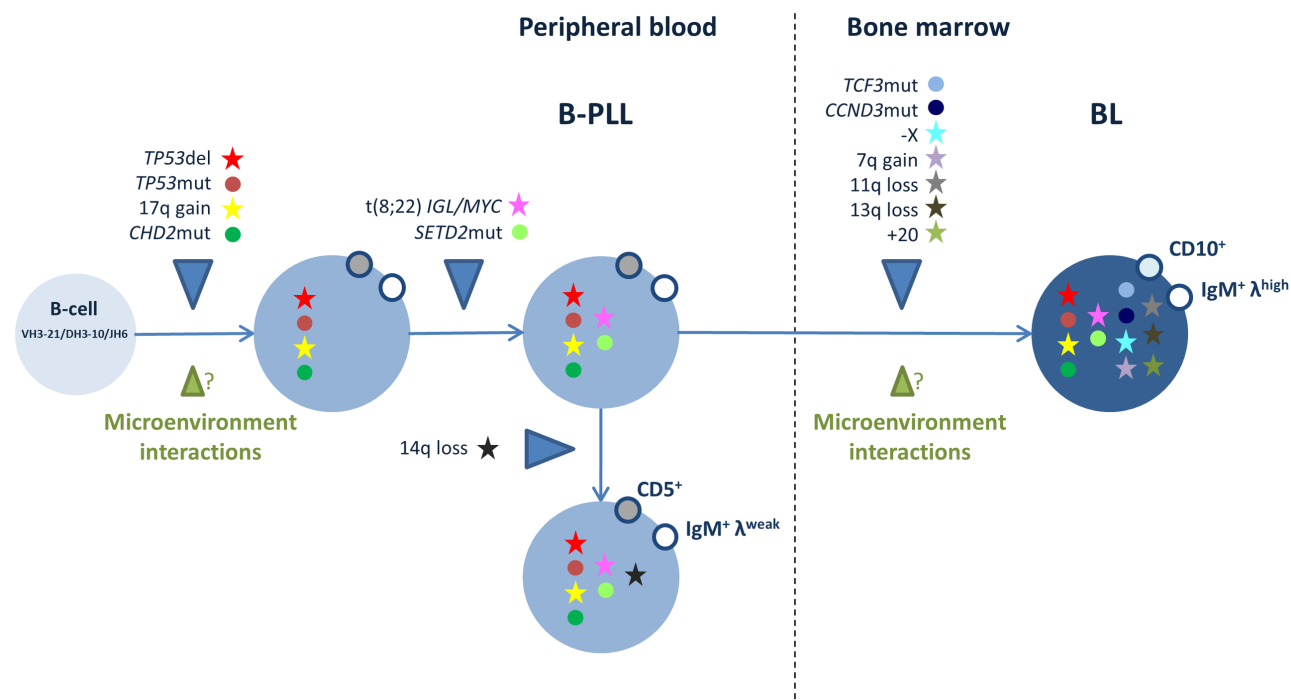

Figure 1. Venn diagram summarizing the biological data.

Figure 2. Hypothetical model of the development of B-PLL and BL in the case described here. The illustration depicts the putative sequential acquisition of chromosomal abnormalities and gene mutations, and the possible role of interactions with the microenvironment. B-PLL = B-cell prolymphocytic leukemia; BL = Burkitt lymphoma.

conserved residue in the proline (P), glutamic acid (E), serine (S), and threonine (T) (PEST) domain, which has a role in the protein's degradation. The great majority of the *CCND3* mutations observed in BL and other B-lymphoid neoplasms target the PEST domain and result in the intracellular accumulation of cyclin D3 and deregulation of the cell cycle.[5] The E555Q *TCF3* mutation, already identified in BL,[5] affects the basic helix–loop–helix domain. Gain-of-function monoallelic mutations in *TCF3* and biallelic inactivating mutations in the *ID3* gene (encoding TCF3's inhibitor) activate B-cell receptor signaling, and thus sustain BL cell survival by engaging the phosphoinositide-3-kinase pathway. These mutations are essentially absent in other mature B-cell malignancies, suggesting that the TCF3/ID3 module has a determining role in the pathogenesis of BL. Indeed, it has been shown that TCF3 contributes to the BL phenotype by enforcing a germinal center-derived transcriptional program; it controls a centroblast-restricted gene expression signature that is "inherited" by BL cells and is intensified in cases with *TCF3/ID3* aberrations.[5] Hence, in the present case, the acquisition of the *TCF3* and *CCND3* mutations may have contributed strongly to the development of BL.

We described a unique chemotherapy-refractory case of de novo high-risk B-PLL with concomitant, clonally related BL. Deregulation of *MYC* is a nonspecific, oncogenic event shared by B-PLL and BL (and other lymphoid malignancies). It is necessary for tumor transformation but does not fully explain the phenotype, which is probably dictated by specific combinations of genetic and epigenetic abnormalities. Clonal evolution, cell migration, disease progression, and drug resistance may all be influenced by the tumor microenvironment.[15] This case further confirms the crucial role of *TCF3* and *CCND3* in BL lymphomagenesis.

Disclosures

The authors have no conflicts of interest to disclose.

Sources of funding

References

1. Chapiro E, Pramil E, Diop M, et al; the Groupe Francophone de Cytogénétique Hématologique (GFCH); the French Innovative Leukemia Organization (FILO). Genetic characterization of B-cell prolymphocytic leukemia: a prognostic model involving MYC and TP53. *Blood*. 2019;134:1821–1831.
2. Dalla-Favera R, Bregni M, Erikson J, et al. Human c-myc onc gene is located on the region of chromosome 8 that is translocated in Burkitt lymphoma cells. *Proc Natl Acad Sci U S A*. 1982;79:7824–7827.
3. Love C, Sun Z, Jima D, et al. The genetic landscape of mutations in Burkitt lymphoma. *Nat Genet*. 2012;44:1321–1325.
4. Richter J, Schlesner M, Hoffmann S, et al; ICGC MMML-Seq Project. Recurrent mutation of the ID3 gene in Burkitt lymphoma identified by integrated genome, exome and transcriptome sequencing. *Nat Genet*. 2012;44:1316–1320.
5. Schmitz R, Young RM, Ceribelli M, et al. Burkitt lymphoma pathogenesis and therapeutic targets from structural and functional genomics. *Nature*. 2012;490:116–120.
6. Nguyen-Khac F, Davi F, Receveur A, et al. Burkitt-type acute leukemia in a patient with B-prolymphocytic leukemia: evidence for a common origin. *Cancer Genet Cytogenet*. 2005;159:74–78.
7. Baptista MJ, Calpe E, Fernandez E, et al. Analysis of the IGHV region in Burkitt's lymphomas supports a germinal center origin and a role for superantigens in lymphomagenesis. *Leuk Res*. 2014;38:509–515.
8. Rossi D, Spina V, Gaidano G. Biology and treatment of Richter syndrome. *Blood*. 2018;131:2761–2772.
9. Asou N, Osato M, Horikawa K, et al. Burkitt's type acute lymphoblastic transformation associated with t(8;14) in a case of B cell chronic lymphocytic leukemia. *Leukemia*. 1997;11:1986–1988.

10. Mohamed AN, Compean R, Dan ME, et al. Clonal evolution of chronic lymphocytic leukemia to acute lymphoblastic leukemia. *Cancer Genet Cytogenet*. 1996;86:143–146.

11. Torelli UL, Torelli GM, Emilia G, et al. Simultaneously increased expression of the c-myc and mu chain genes in the acute blastic transformation of a chronic lymphocytic leukaemia. *Br J Haematol*. 1987;65:165–170.

12. Maeshima AM, Taniguchi H, Toyoda K, et al. Clinicopathological features of histological transformation from extranodal marginal zone B-cell lymphoma of mucosa-associated lymphoid tissue to diffuse large B-cell lymphoma: an analysis of 467 patients. *Br J Haematol*. 2016;174:923–931.

13. Pasqualucci L, Khiabanian H, Fangazio M, et al. Genetics of follicular lymphoma transformation. *Cell Rep*. 2014;6:130–140.

14. Schmitz R, Ceribelli M, Pittaluga S, et al. Oncogenic mechanisms in Burkitt lymphoma. *Cold Spring Harb Perspect Med*. 2014;4:a014282.

15. Mangolini M, Ringshausen I. Bone marrow stromal cells drive key hallmarks of B cell malignancies. *Int J Mol Sci*. 2020;21:E1466.

<div align="center">**Supplementary Information**</div>

Methods

Cell sorting and DNA extraction

The peripheral blood (PB) and bone marrow (BM) samples used for whole exome sequencing and targeted deep sequencing were obtained from cryopreserved mononuclear cells. The CD19+/CD5+ B-cells and CD3+ T-cells from PB were sorted as described previously.[1] The purity of the cell fractions assessed by flow cytometry was 99.8% for the CD19+/5+ cells and 97.9% for the CD3+ cells. A morphological assessment and flow cytometry showed that 87% of the lymphocytes in the BM were Burkitt cells. DNA was extracted from PB sorted cell fractions and BM sample using the All Prep DNA/RNA kit (Qiagen, Courtaboeuf, France), according to the manufacturer's recommendations.

Whole Exome Sequencing (WES)

WES was performed as described previously.[2] Briefly, exome capture was performed with the SureSelect V5 Mb All Exon Kit (Agilent Technologies, Les Ulis, France) following the standard protocols. Paired-end sequencing (2 x 100 bp) was performed using HiSeq2000 sequencing instruments (Illumina, San Diego, CA). The mean coverage in the targeted regions was 89X for the CD19+/5+ cells, 88X for the CD3 cells and 141X for the BM cells. Reads were mapped to the reference genome hg19 using the Burrows–Wheeler Aligner (BWA) alignment tool version 0.7.10. PCR duplicates were removed using Picard Tools - MarkDuplicates (1.119). Local realignment around indels and base quality score recalibration were performed using GATK 3.2 (Genome Analysis ToolKit). Reads with a mapping quality score < 30 were ignored. SNVs and indels were called with VarScan2 somatic 2.3.7. The null hypothesis of equal allele frequencies between tumor and reference was tested using the two-tailed Fisher exact test. The variants were adopted as candidate mutations when P value was <0.01 and allele frequency was <0.1 in the reference sample. Variants were annotated with Annovar. We excluded synonymous single nucleotide variants (SNVs), variants located in intergenic, intronic, untranslated regions and non-coding RNA regions, and removed variants with mapping ambiguities. The effect of the mutation was predicted by SIFT (http://sift.jcvi.org/) and PolyPhen2 (http://genetics.bwh.harvard.edu/pph2/) algorithms. Mutations were searched in Catalogue of Somatic Mutations in Cancer database (http://cancer.sanger.ac.uk/cosmic/) and in dbSNP version 129. Somatic copy number variations (CNV) were identified with Control-FREEC (v9.1).

Targeted deep sequencing

Targeted deep sequencing was performed as described previously.[2] Primers flanking exons containing candidate somatic variants were designed using Primer3

(http://frodo.wi.mit.edu/primer3/). Short fragments of 100 to 200 bp were PCR-amplified from genomic DNA and were subsequently pooled for library construction. Amplicon libraries were sequenced in an Illumina MiSeq flow cell using the onboard cluster method, as paired-end sequencing (2x150 bp reads) (Illumina, San Diego, CA). The mean coverage was 2110X. Quality of reads was evaluated using FastQC 0.11.2. (http://www.bioinformatics.bbsrc.ac.uk/projects/fastqc/). Reads were mapped to the reference genome hg19 using the Burrows–Wheeler Aligner (BWA) alignment tool version 0.7.10. Local realignment around indels and base quality score recalibration were performed using GATK 3.2 (Genome Analysis ToolKit). SNVs and indels were called with VarScan2 somatic 2.3.7.

References

1. Damm F, Mylonas E, Cosson A, et al. Acquired initiating mutations in early hematopoietic cells of CLL patients. *Cancer discovery.* 2014;4(9):1088-1101.
2. Chapiro E, Pramil E, Diop M, et al. Genetic characterization of B-cell prolymphocytic leukemia: a prognostic model involving MYC and TP53. *Blood.* 2019;134(21):1821-1831.

Supplemental Table 1. List of the variants detected by whole exome sequencing in CD19+/CD5+ peripheral blood and bone marrow samples. (Excel file – see SDC http://links.lww.com/HS/A155).
The first tab contains the full dataset and the second tab contains a summary.

Supplemental Table 2. Copy number aberrations >5 Mb from whole exome sequencing. The regions are described according to the hg19 reference genome.

Sample	Chromosome	Bands	Start	End	Length (Mb)	Gain or loss
CD19+/CD5+ blood cells	14	q23.3-q31.1	66082543	81737252	15.6	loss
	17	p13.3-p11.2	5903	18997018	18.9	loss
	17	q23.1-q24.3	58177985	69335064	11.1	gain
Bone marrow cells	7	q11.22-q21.11	69364152	77584433	8.2	gain
	7	q22.1-q36.3	102136461	158937536	56.8	gain
	11	q23.3-q25	119077082	134257987	15.1	loss
	13	q32.3-q34	99738352	115070490	15.3	loss
	17	p13.3-p11.2	5903	18997018	18.9	loss
	17	q23.1-q25.3	58288598	81052464	22.7	gain
	20	p13-q13	68159	62904965	62.8	gain
	X	p22-q28	200749	154775068	154.5	loss

Gene	Mutation type	Mutation	Chromosome	Position	Blood (B-PLL) VAF	Bone marrow (BL) VAF	sift score	polyphen score	dbsnpID(r129)	COSMIC
TP53	missense	TP53:NM_000546:exon8:c.T824A:p.L275Q	chr17	7577114	95,83	84,48	NA	1	NA	http://cancer.sanger.ac.uk/cosmic/mutation/overview?id=10893
JUP	missense	JUP:NM_021991:exon11:c.C1853T:p.A618V	chr17	39913957	55,79	36,96	NA	0,838	NA	
IL6ST	missense	IL6ST:NM_002184:exon17:c.T2485G:p.S829A	chr5	55237182	54,55	45	0,3	0,588	NA	
TMPO	missense	TMPO:NM_003276:exon4:c.C1025T:p.P342L	chr12	98927060	54,24	44,14	0,08	0	NA	
ZNF134	missense	ZNF134:NM_003435:exon3:c.A803G:p.Y268C	chr19	58132290	52,68	45,82	0,18	0,987	NA	
ADAM30	missense	ADAM30:NM_021794:exon1:c.C1396A:p.L466I	chr1	120437564	52,27	35,27	NA	0,993	NA	
DES	missense	DES:NM_001927:exon1:c.C65T:p.P22L	chr2	220283249	52,03	42,01	NA	0,43725	NA	
OR51E1	missense	OR51E1:NM_152430:exon2:c.T18G:p.N6K	chr11	4673774	50	40,43	NA	0,264	NA	
NFASC	missense	NFASC:NM_001005388:exon18:c.G1930A:p.V644M	chr1	204948149	47,54	48,97	NA	0,921	NA	
CHD2	frameshift deletion	CHD2:NM_001271:exon33:c.4160_4178del:p.P1387Rfs*13	chr15	93545429	47,06	35,95	NA	NA	NA	
MSH6	missense	MSH6:NM_000179:exon1:c.C71T:p.S24L	chr2	48010443	46,59	51,45	0,22	0,008	NA	
CSMD2	missense	CSMD2:NM_052896:exon65:c.G9808T:p.G3270W	chr1	33990638	45,87	40,21	NA	0,648	NA	
COL27A1	missense	COL27A1:NM_032888:exon10:c.C2237T:p.P746L	chr9	116968545	45,81	44,94	0,09	1	NA	
MYOT	missense	MYOT:NM_001135940:exon9:c.A732C:p.E244D	chr5	137222646	44,44	40,61	NA	0,465	NA	
FZD6	missense	FZD6:NM_001164615:exon4:c.A1179C:p.L393F	chr8	104337513	44,3	41,47	NA	0,853	NA	
SORL1	missense	SORL1:NM_003105:exon25:c.C3514T:p.R1172C	chr11	121448043	39,7	74,09	0,11	0,999	NA	
SETD2	frameshift insertion	SETD2:NM_014159:exon3:c.2628_2629insAG:p.G878Qfs*14	chr3	47163498	34,88	47,58	NA	NA	NA	
TET2	frameshift deletion	TET2:NM_001127208:exon9:c.4179_4182del:p.1393_1394del	chr4	106190901	34,02	28,17	NA	NA	NA	
BNIP2	missense	BNIP2:NM_004330:exon6:c.A886G:p.M296V	chr15	59964888	29,9	47,64	NA	0,904	NA	
HIST1H4K	missense	HIST1H4K:NM_003541:exon1:c.G223C:p.E75Q	chr6	27799083	0	50	NA	0,784	NA	
NFATC1	splice site	NA	chr18	77156352	0	50	NA	NA	NA	
HLA-B	missense	HLA-B:NM_005514:exon3:c.T466C:p.S156P	chr6	31324097	0	47,62	NA	0,403143	NA	
C9orf5	missense	C9orf5:NM_032012:exon18:c.A2606T:p.D869V	chr9	111782774	0	45,98	NA	0,941	NA	
MFSD7	missense	MFSD7:NM_032219:exon7:c.T844G:p.F282V	chr4	677547	0	43,9	NA	0,869	NA	
RQCD1	missense	RQCD1:NM_005444:exon3:c.C260G:p.S87C	chr2	219447749	0	43,88	NA	0,997	NA	http://cancer.sanger.ac.uk/cosmic/mutation/overview?id=247126
FNDC3B	missense	FNDC3B:NM_001135095:exon15:c.T1643C:p.L548P	chr3	172052735	1,55	42,56	NA	0,983	NA	
COQ5	missense	COQ5:NM_032314:exon7:c.A935G:p.E312G	chr12	120941636	0	42,3	NA	0,79	NA	
LATS2	missense	LATS2:NM_014572:exon4:c.T743C:p.L248P	chr13	21563176	0	40,91	0,25	0,953	NA	
TCF3	missense	TCF3:NM_001136139:exon17:c.G1663C:p.E555Q	chr19	1612356	0	40,53	NA	NA	NA	
ADARB1	missense	ADARB1:NM_015834:exon10:c.T1847C:p.L616P	chr21	46624631	0	40,35	NA	0,928	NA	
SLC6A5	missense	SLC6A5:NM_004211:exon15:c.G2145C:p.M715I	chr11	20673909	0	40,31	0,23	0,366	NA	
SRRM4	missense	SRRM4:NM_194286:exon7:c.C571T:p.R191W	chr12	119563241	0	39,45	NA	NA	NA	http://cancer.sanger.ac.uk/cosmic/mutation/overview?id=1359214
IARS	missense	IARS:NM_013417:exon29:c.C3146T:p.S1049L	chr9	95004467	0	38,98	0,05	0	NA	
ADAMTS3	missense	ADAMTS3:NM_014243:exon10:c.A1454G:p.D485G	chr4	73184320	0,9	38,78	NA	0,999	NA	
CACNA1D	missense	CACNA1D:NM_000720:exon48:c.A5983T:p.S1995C	chr3	53844056	0	38,2	NA	0,588	NA	
MYO3A	splice site	NA	chr10	26491891	0	37,43	NA	NA	NA	
CCND3	missense	CCND3:NM_001760:exon5:c.T875A:p.L292Q	chr6	41903682	0	37,25	NA	0,831	NA	
MYO3A	missense	MYO3A:NM_017433:exon34:c.A4589G:p.Q1530R	chr10	26491895	0	37,08	0,14	0,629	NA	
MASP1	missense	MASP1:NM_001879:exon12:c.G1511A:p.R504H	chr3	186944239	0	36,71	0,27	0,50478	NA	
KIAA1244	missense	KIAA1244:NM_020340:exon33:c.G5503A:p.E1835K	chr6	138655486	0	36,43	0,15	NA	NA	
OR52N1	missense	OR52N1:NM_001001913:exon1:c.G468C:p.M156I	chr11	5809579	0	36,33	0,41	0,004	NA	
SOX11	nonframeshift deletion	SOX11:NM_003108:exon1:c.672_677del:p.224_226del	chr2	5833525	0	36,03	NA	NA	NA	http://cancer.sanger.ac.uk/cosmic/mutation/overview?id=1009262
LRP2	missense	LRP2:NM_004525:exon10:c.G1103A:p.R368H	chr2	170139451	0	34,9	0,2	0	NA	
HLA-C	stoppain	HLA-C:NM_002117:exon5:c.C907T:p.Q303X	chr6	31237851	0	34,17	NA	0,241364	NA	
EXD3	missense	EXD3:NM_017820:exon17:c.G1849A:p.V617M	chr9	140242672	0	31,65	0,39	NA	NA	
CASP2	missense	CASP2:NM_001224:exon9:c.A880G:p.I294V	chr7	142997478	0	27,85	NA	NA	NA	

B-PLL: B-cell prolymphocytic leukemia; BL: Burkitt lymphoma

in blue mutations detected in both B-PLL and BL cells
in black mutations detected in BL cells only
in bold recurrent mutations in **B-PLL** or **BL**